RESEARCH ARTICLE | MARCH 31 2020

Development of MCSF (M=La, Ba) cathode materials for proton conducting fuel cell application FREE

Nafisah Osman ✉; Nurul Izzati Abd Malek; Ismariza Ismail; Anisah Shafiqah Habiballah; Abdul Mutalib Md Jani

AIP Conf. Proc. 2221, 020001 (2020)
https://doi.org/10.1063/5.0003786

Development of MCSF (M=La, Ba) Cathode Materials for Proton Conducting Fuel Cell Application

Nafisah Osman[1,2,a)], Nurul Izzati Abd Malek[2,b)], Ismariza Ismail[3,c)], Anisah Shafiqah Habiballah[2, d)] and Abdul Mutalib Md Jani[2,4,e)]

[1] *Faculty of Applied Sciences, Universiti Teknologi MARA, 02600 Arau, Perlis, Malaysia.*
[2] *Proton Conducting Fuel Cell Research Group, Faculty of Applied Sciences, Universiti Teknologi MARA, 40450 Shah Alam, Selangor, Malaysia*
[3] *Faculty of Engineering Technology, Universiti Malaysia Perlis, 02100 Padang Besar, Perlis, Malaysia*
[4] *Faculty of Applied Sciences, Universiti Teknologi MARA, 35400 Tapah, Perak, Malaysia.*

[a)]Corresponding author: fisha@uitm.edu.my
[b)]izzatimalek45@gmail.com
[c)]is_mariza@yahoo.com
[d)]anisahhabiballah7407@gmail.com
[e)]abdmutalib@uitm.edu.my

Abstract. Two cathode materials for proton-conducting fuel cell (PCFC), $La_{0.6}Sr_{0.4}Co_{0.2}Fe_{0.8}O_{3-\delta}$ (LSCF) and $Ba_{0.5}Sr_{0.5}Co_{0.8}Fe_{0.2}O_{3-\delta}$ (BSCF) were investigated regarding their microstructural and electrical properties under air containing atmosphere. The respective sample was prepared via a modified sol-gel method using an activated carbon as a dispersing agent and anodic aluminium oxide (AAO) templating method assisted with sol-gel process. The powders were subjected to X-ray Diffractometer (XRD) and Brunauer-Emmet-Teller (BET). A symmetrical half-cell of LSCF|BCZY|LSCF and BSCF|BCZY|BSCF (BCZY = $BaCe_{0.54}Zr_{0.36}Y_{0.1}O_{2.95}$)was fabricated and characterized using an electrochemical impedance spectroscopy (EIS) and scanning electron microscope (SEM). After calcined at T= 900 °C, both of the LSCF and BSCF demonstrated their single-phase structure and exhibited highly dispersed powders with large surface area as proven by BET result. For electrical analyses, impedance spectrum of the cathodes was referred only to the two main contributions of cathode responses which were charge transfer at cathode/electrolyte interface and oxygen adsorption/dissociation on the cathode surface. At 600 °C, the polarization resistance of LSCF half-cell (R_p = 4.94 Ω.cm^2) was comparable to BSCF (R_p =4.50 Ω.cm^2). SEM images revealed no delamination along the electrolyte/ electrode interface after EIS measurements as no sign of crack was observed for both samples. It can be concluded that the microstructure of the cathode layer can be tailored by altering the sample's preparation route which in turn to enhance the PCFC performance.

INTRODUCTION

Solid oxide fuel cell (SOFC) is a promising future power generation system that produces electricity via redox reaction process using fuel and oxidant gases. A conventional SOFC made up of perovskite type oxide ceramics material that carries dominantly anionic charge at the electrolyte and electronic charge species at the electrodes. The SOFC shows high ionic conductivity of ~1 Scm^{-1} at high temperature regions (800°C to 1000°C) but creates severe issues to the system such as chemical instability during cell operation, thermo-mechanical failure in the component and difficulties in choosing sealant [1- 4]. These problems can be solved by reducing the operating temperature to intermediate range (600°C-800°C) and one of the approaches is developing new electrolyte material containing protonic charge carrier species known as proton conducting fuel cell (PCFC).

The PCFC is a green technology system that operates at intermediate temperature lead to rapid start-up materials and saving the total operating cost [5, 6]. The removal of water content at the cathode site causes less fuel dilution

The 1st International Conference on Physics and Applied Physics (The 1st ICP&AP) 2019
AIP Conf. Proc. 2221, 020001-1–020001-5; https://doi.org/10.1063/5.0003786
Published by AIP Publishing. 978-0-7354-1980-3/$30.00

because water is swept away by air [7]. Proton conductor also exhibits low activation energy (E_a) compared to the conventional SOFC. Lowering the E_a increases mechanical and chemical stability that give rise to high conductivity [8]. However, the biggest problem found in PCFC especially at the cathode site is the high polarization resistance (R_p) that reduces the overall system [9]. Thus, selection of the best material in this electrochemical reaction system is important in order to reduce its drawbacks. One of the approaches that have been made is by reducing the particle size to nanosize range to increase the surface active area for high electrochemical performance [10]. In this study, $La_{0.6}Sr_{0.4}Co_{0.2}Fe_{0.8}O_{3-\delta}$ (LSCF) and $Ba_{0.5}Sr_{0.5}Co_{0.8}Fe_{0.2}O_{3-\delta}$ (BSCF) cathodes nanoparticles were synthesized via a sol-gel method with the aid of dispersing agent and template-assisted, respectively. The electrolyte-supported half-cell was then fabricated via a dry pressing and spin coating techniques followed by an electrochemical performance of the cathode material. Introducing these additives during powder's preparation is expected to tailor the microstructure of cathode material and become one of promising approaches to produce a high power generation system.

METHODOLOGY

A stoichiometric amount of lanthanum, strontium, cobalt, and iron nitrate-based salts were dissolved in 100 mL deionized water. Citric acid and ethylenediaminetetraacetic acid (EDTA) was added to the solution then subjected to double-boiled process until a clear solution formed. A small amount of activated carbon that served as a dispersing agent was added to the solution in order to promote the dispersion of sol particles. The mixture was pre-heated at 180°C under continuous strirring until became a black gel. The gel was dried in a venticell oven at 100°C for 12 hours. Then, the dried powder was grinded and calcined at 900°C for 5 hours with the rate of 10°C/minutes to obtain a single phase LSCF. The same procedures were repeated for the preparation of BSCF. The anodic aluminium oxide (AAO) was then fabricated and undergone several processing steps to get a BSCF nanotubes as reported by Habiballah et al [11]. All the powders were subjected to X-ray diffraction (XRD) and Brunauer-Emmet-Teller (BET) analyses.

In order to study the electrochemical performance of the cathode compounds, the BCZY powder was prepared via a modified sol-gel method as reported by Abdullah et al [12] and then sintered to become electrolyte-supported. The prepared cathode powders were then formulated into slurry using a mixture of ethyl cellulose and terpineol that served as a binder. The slurry was then coated on both surfaces of the BCZY pellet with 2000 rpm for 30 seconds and further sintered at 900°C for 1 hour. The symmetrical half-cell of LSCF|BCZY| LSCF and BSCF|BCZY| BSCF were then coated with platinum (Pt) as a current collector before starting up the electrochemical impedance spectroscopy (EIS) measurement in air containing atmosphere. The measurement was performed using ZIVE SP2 Electrochemical Workstation with 10 mV AC signal applied and the frequency ranging from 1MHz to 10 mHz. The impedance spectrum was recorded from 400°C to 800°C at 50°C interval and then fitted using ZMAN™ 2.2 f3 software. Finally, the morphology of the half-cell after the EIS testing was observed using a Scanning Electron Microscope (SEM).

RESULTS AND DISCUSSION

X-ray diffraction (XRD)

Figure 1 shows the XRD patterns for both LSCF and BSCF after calcined at 900°C.As reported by Ismail et al [13], single phase of the LSCF cathode started to appear at T= 700˚C and almost completely formed at T= 900˚C. The same temperature was also observed for the complete formation of BSCF single phase compound. All the main peaks in both XRD patterns were matched with Joint Committee of Powder Diffraction Standards (JCPDS) file number JCPDS 01-089-1268 for LSCF and JCPDS-01-082-2445 for BSCF with orthorhombic and cubic structures, respectively. The prominent peaks were indexed based on their Miller Indices (hkl) of LSCF at (110), (020), (202), (220), (132), (224), (332) and BSCF at (100), (110), (111), (200), (210), (211), (220), (310). The values of lattice constant for both of the samples are in good agreement with the pattern list of LSCF (a=5.4750Å; b=5.5360Å; c=7.8480Å) and BSCF (a=3.8491Å; b=3.8491Å; c=3.8491Å) as shown in Table 1. Thus, no significant changes in lattice parameter was observed indicating that the materials have achieved phase stability at 900°C and the synthesis route is not a dominant factor that affect the phase formation of the materials [14].

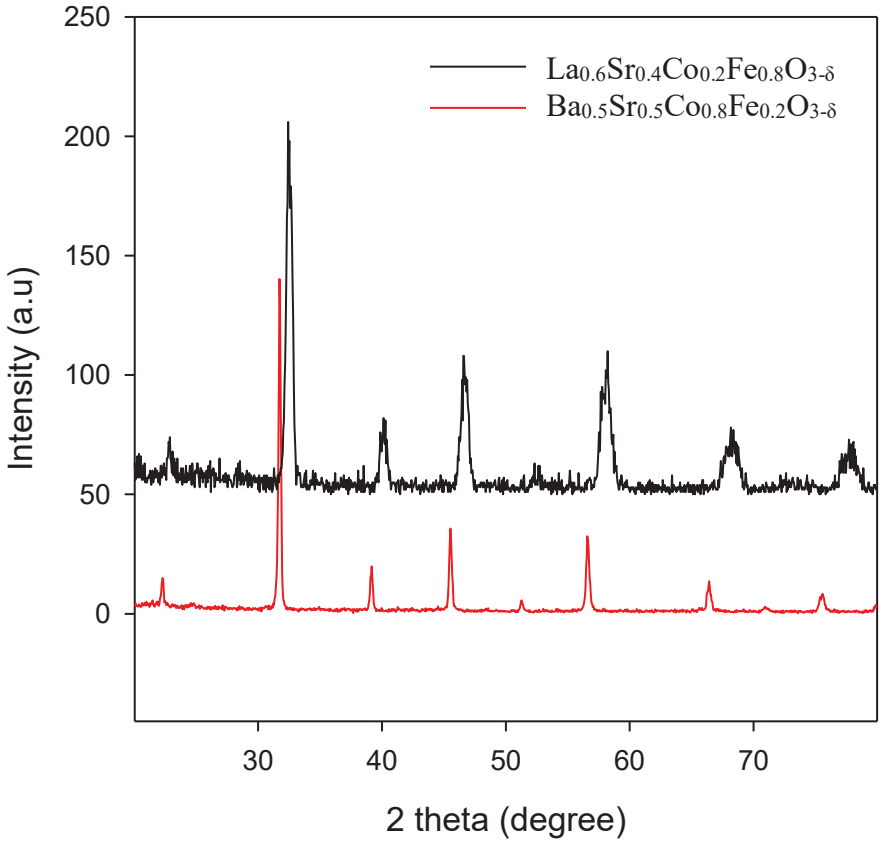

FIGURE 1.XRD pattern of the cathode samples after calcined at 900˚C.

TABLE 1. Calculated lattice constant of LSCF and BSCF powders after calcined at 900ºC.

Sample name	Microstructural aid	Lattice constant (Å)
$La_{0.6}Sr_{0.4}Co_{0.2}Fe_{0.8}O_{3-\delta}$	Activated carbon (AC)	a= 5.4840 b= 5.5270 c= 7.8230
$Ba_{0.5}Sr_{0.5}Co_{0.8}Fe_{0.2}O_{3-\delta}$	Anodic Aluminium Oxide (AAO)	a= 3.8490 b= 3.8490 c= 3.8490

Brunauer-Emmet-Teller (BET)

The specific surface area obtained from the BET analysis using nitrogen adsorption and desorption method were 11.02 m^2/g and 9.28 m^2/g for LSCF and BSCF, respectively as shown in Table 2. Clearly seen the specific surface area of respective LSCF and BSCF using each of the modified sol-gel method was higher as compared to others route. Thus, both of methods used have the ability to disperse particles to form an ultrafine cathode powders. As reported by Samat et al., [15], the high surface area for cathode samples is very important since it can increase the number of active site for oxygen reduction reaction (ORR).

TABLE 2. Comparison of the specific surface area for cathode materials prepared using different synthesizing methods

Sample ID	Method	BET (m^2/g)	Reference
$La_{0.6}Sr_{0.4}Co_{0.2}Fe_{0.8}O_{3-\delta}$	Acetate method	8.30	[16]
$La_{0.6}Sr_{0.4}Co_{0.2}Fe_{0.8}O_{3-\delta}$	Citrate method	5.50	[17]
$Ba_{0.5}Sr_{0.5}Co_{0.8}Fe_{0.2}O_{3-\delta}$	EDTA-citrate method	5.56	[18]
$Ba_{0.5}Sr_{0.5}Co_{0.8}Fe_{0.2}O_{3-\delta}$	Sol-gel combined citrate-EDTA complexing method	2.40	[19]
$Ba_{0.5}Sr_{0.5}Co_{0.8}Fe_{0.2}O_{3-\delta}$	Template-assisted sol-gel method	9.28	[This work]
$La_{0.6}Sr_{0.4}Co_{0.2}Fe_{0.8}O_{3-\delta}$	Activated carbon-assisted sol-gel method	11.02	[This work]

Electrochemical Impedance Spectroscopy (EIS)

Figure 2 shows the EIS spectra for both LSCF and BSCF half-cell recorded in air containing atmosphere at 600°C using BCZY electrolyte as a support. Both spectra were well fitted with an equivalence circuit of Rs(R1Q1)(R2Q2) as inset in Fig. 2. The arcs with respective circuit contribute a significant finger print to the cathode reaction processes. The Rs refers to electrolyte responses, which was manifested as ohmic resistance [16, 17]. The first arc of R1Q1 represents the cathode process at middle frequency regime which indicates the ionic charge transfer reaction at the electrode to electrolyte layer. R2Q2 represents the cathode reaction process at low frequency semicircle that assigned to oxygen dissociation and adsorption process at the cathode surface [18, 19]. It is also observed that the increasing in frequency lead to the reduction of the resistance values and the arc became small. Thus, the adsorption, dissociation and diffusion processes of oxygen species probably limited the cathode reaction at 600°C as pointed by the Adler-Lane-Steele model [20-21].

The main purpose of fitting process is to determine the polarization resistance, R_p. The lowest R_p signifies the microstructure modification of the prepared samples lead to lengthen of surface active area for vast performance. The LSCF and BSCF exhibited R_p of 4.94 Ωcm^2 and 4.50 Ωcm^2, respectively which proven that the microstructural modification using an activated carbon as a dispersing agent and AAO template-assisted method have successfully produced a nanoceramic cathode powders. These results were in-line with the study by B. He et al., [23] and Zhao et al., [24] that works on the same material.

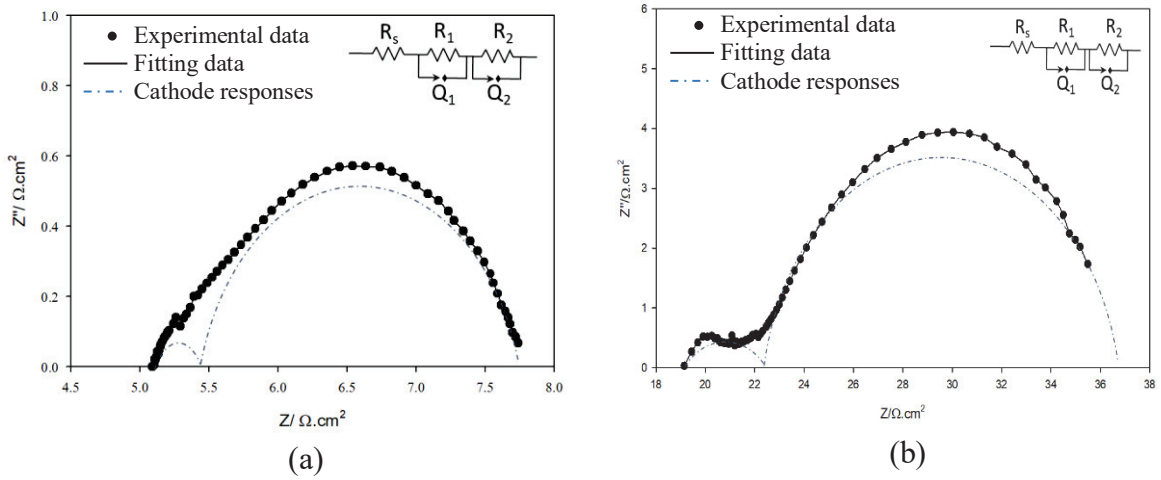

FIGURE 2. Nquist plot with its corresponding equivalent circuit of a symmetrical half-cell of (a) LSCF and (b) BSCF measured at 600°C under air containing atmosphere.

Scanning electron microscope (SEM) analysis

Figure 3 demonstrated the SEM images of the fractured pellet for both LSCF and BSCF samples. Clearly seen the layers between electrolyte and cathode are well attached with each other with no sign of crack and delamination.

These cathode microstructures still preserved after EIS testing, signifying no detrimental effect on the cell structure during longer operating time. A good adhesion between electrolyte and electrode also resulted to a low contact resistance of the half-cell.

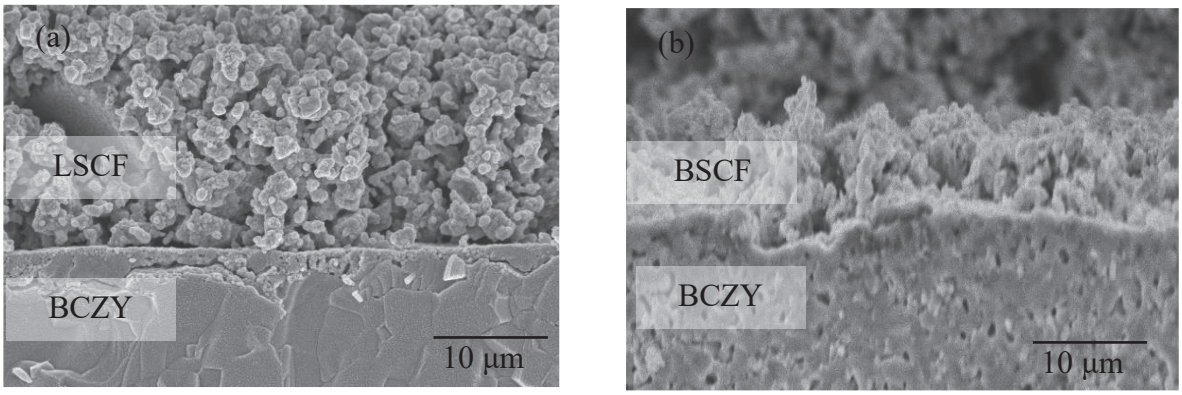

FIGURE 3. SEM images of the cross-sectional half-cell of (a) LSCF and (b) BSCF couple with BCZY electrolyte after the EIS operating temperatures (400-800°C).

CONCLUSION

The ultrafine LSCF and BSCF powders was successfully synthesized using a modified sol-gel method with the help of activated carbon as dispersing agent and AAO-templating method, respectively. These routes gave a remarkable impact in tailoring the microstructure to nanosize ranges for high surface active site of respective LSCF and BSCF materials. Production of ultrafine cathodes powders also promotes to a good contact between electrolyte and cathode.

ACKNOWLEDGEMENTS

This work was supported by The Ministry of Education under Fundamental Research Grant Scheme (600-IRMI/FRGS 5/3 (035/2017)) and Universiti Teknologi MARA for the facilities and supports.

REFERENCES

1. J. Huang, F. Xie, C. Wang, and Z. Mao, *Int. J. Hydrogen Energy* **37**, 877–883 (2012).
2. E. D. Wachsman and K. T. Lee, *Science* **334**, 935–939 (2011).
3. H. Yokokawa, N. Sakai, T. Horita, K. Yamaji, M. E. Brito, and H. Kishimoto, *J. Alloys Compd.* **452**, 41–47 (2008).
4. S. Tao and J. T. S. Irvine, *Nat. Mater.* **2**, 320-325 (2003).
5. S. Hossain, A. M. Abdalla, S. N. B. Jamain, J. H. Zaini, and A. K. Azad, *Renew. Sustain. Energy Rev.***79**, 750–764 (2017).
6. E. Fabbri, L. Bi, D. Pergolesi, and E. Traversa, *Adv. Mater.* **24**, 195–208 (2012).
7. Z. Wang, W. Yang, S.P. Shafi, L. Bi, Z. Wang, *J. Mater. Chem. A.***3**, 8405–8412 (2015).
8. R. Peng, T. Wu, W. Liu, X. Liu, and G. Meng, *J. Mater. Chem.***20**, 6218–6225 (2010).
9. M. Shang, J. Tong, and R. O'Hayre, *RSC Adv.***3**, 15769–15775 (2013).
10. S. M. Babiniec, S. Ricote, and N. P. Sullivan, *J. Electrochem. Soc.***161**, F717–F723 (2014).
11. N. A. Abdullah, S. Hasan, and N. Osman, *J. Chem.* **2013**, (2012).
12. A. S. Habiballah, N. Osman, and A. M. M. Jani, "A new route of synthesizing perovskite nanotubes by templating approach," in AIP Conference Proceedings 1877, pp. 30006.
13. M. Arnold, T. M. Gesing, J. Martynczuk, and A. Feldhoff, *Chem. Mater.***20**, 5851–5858 (2008).
14. W. D. Yang, Y.-H. Chang, and S.-H. Huang, *J. Eur. Ceram. Soc.***25**, 3611–3618 (2005).
15. M A. A. Samat, M. R. Somalu, A. Muchtar, O. H. Hassan, and N. Osman, *J. Sol-Gel Sci. Technol.***78**, 382–393 (2016).
16. I. Ahmed, S.G. Eriksson, E. Ahleberg, C.S. Knee, M. Karlsson, *Solid State Ionics* **177**, 2357–2362 (2006).
17. D. A. Stevenson, N. Jiang, R. M. Buchanan, and F. E. G. Henn, *Solid State Ionics* **62**, 279–285 (1993).
18. J. Dailly, F. Mauvy, M. Marrony, M. Pouchard, and J.-C. Grenier, *J. Solid State Electrochem.***15**, 245–251 (2011).
19. S. Ricote, N. Bonanos, P. M. Rørvik, and C. Haavik, *J. Power Sources* **209**, 172–179 (2012).
20. S.W. Baek, J. Bae, and Y.-S. Yoo, *J. Power Sources* **193**, 431–440 (2009).
21. J. H. Kim, M. Cassidy, J. T. S. Irvine, and J. Bae, *Chem. Mater.* **22**, 883–892 (2009).
22. S. B. Adler, *Solid State Ionics* **111**, 125–134 (1998).
23. B. He, L. Zhang, D. Ding, J. Xu and Y. Ling, *J. Power Sources* **287**, 170–176 (2015).
24. L. Zhao, B. He, Z. Xun, R. Peng, G. Meng, and X. Liu, *Int. J. Hydrogen Energy* **35**, 3769–3774 (2010).